

Thermal regulation of building-integrated concentrating photovoltaic system using phase change material

Cite as: AIP Conference Proceedings **1766**, 090001 (2016); <https://doi.org/10.1063/1.4962107>
Published Online: 01 September 2016

Idris Al Siyabi, Shivangi Sharma, Tapas K. Mallick, et al.



View Online



Export Citation

ARTICLES YOU MAY BE INTERESTED IN

[Thermal analysis of a multi-layer microchannel heat sink for cooling concentrator photovoltaic \(CPV\) cells](#)

AIP Conference Proceedings **1881**, 070001 (2017); <https://doi.org/10.1063/1.5001434>

[Electricity enhancement and thermal energy production from concentrated photovoltaic integrated with a 3-layered stacked micro-channel heat sink](#)

AIP Conference Proceedings **2012**, 080001 (2018); <https://doi.org/10.1063/1.5053529>

[Photovoltaic system integrated with phase change material for South west UK climate](#)

AIP Conference Proceedings **2012**, 080007 (2018); <https://doi.org/10.1063/1.5053535>

Lock-in Amplifiers
up to 600 MHz



Zurich
Instruments



Thermal Regulation of Building-Integrated Concentrating Photovoltaic System using Phase Change Material

Idris Al Siyabi^{1,*}, Shivangi Sharma¹, Tapas K. Mallick¹ and Senthilarasu Sundaram¹

¹*Environment and Sustainability Institute, University of Exeter, Penryn Campus, Cornwall TR109FE, UK*

*Corresponding author: ia257@exeter.ac.uk

Abstract. Thermal regulation of building-integrated concentrating photovoltaic (BICPV) systems have a direct influence on the photovoltaic performance. This paper investigates the thermal behavior of a BICPV and phase change material (PCM) system through numerical modeling simulations. Based on an updated mathematical model, theoretical simulation has been conducted for a BICPV-PCM system. The results show a 3% electrical efficiency improvement of the BICPV-PCM system in certain cases.

INTRODUCTION

Concentrated photovoltaic (CPV) technology has attracted a considerable amount of research focus, and is in the early stages of commercialization. The electrical generation of installed CPV systems has increased rapidly from 2MW in 2007 to around 1800 MW in 2015[1].

CPV technology concentrates solar irradiation into a small spot as shown in figure 1, which allows more radiation on the solar cell to be harvested compared to non-concentrated systems. Thus, CPV technology has the advantage of requiring less cell area and fewer materials than conventional photovoltaic.

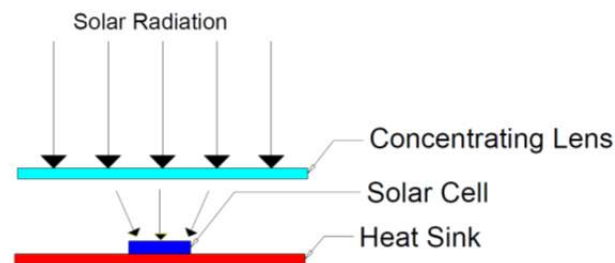


FIGURE 1. Typical CPV system arrangement.

The concentrated solar radiation that is received by the solar cell is reflected, transmitted (through the solar cell) or absorbed. The amounts of reflected and transmitted solar radiation are very small as compared to that which is absorbed. The level of absorption varies according to the band gap of the semiconductor, with only an estimated 16% of the solar energy received by the solar cell being used to generate electricity. The remaining 84% is converted into heat[2].

Integration of renewable energy resources into buildings and improving energy efficiency reduce the energy utilization within buildings and increase sustainability. Building integrated concentrated photovoltaic (BICPV) systems offer advantages over conventional building integrated photovoltaics by improving electrical conversion, reducing heat loss and requiring less space. The BICPV system consists of optical concentrators, a photovoltaic

receiver and a heat sink. A tracking mechanism is not recommended for low concentration photovoltaics (LCPV) due to high capital, operation and maintenance costs. Conventional crystalline silicon photovoltaics are more common in low concentration levels due to their low cost and reasonable performance.

As mentioned earlier, the PV is exposed to high temperatures in a CPV system due to the higher concentration of solar radiation. This excessive heat in the solar cell must be removed to avoid efficiency drop, rapid cell efficiency degradation or even permanent cell damage. There are two different approaches to cool the solar cells: passive or active. The passive approach uses natural phenomena such as conduction and convection to cool the solar cell. This is a valuable cooling technique due to its low capital, operation and maintenance costs [1]. The active approach uses mechanical means such as pumps or fans to circulate the cooled fluid (Water or Air) into the system. This is considered very efficient. The extracted heat from the CPV can be used for domestic heating. However, active cooling is complicated, more costly in terms of construction, operation and maintenance. More detail on cooling concentrated photovoltaic systems can be found in [4].

Phase change material (PCM) is a passive approach to photovoltaic thermal regulation that has been studied widely. The main characteristic of PCM is high latent heat capacity. This feature enables the materials to absorb heat during the phase change stage. In a typical PV-PCM application, the phase change materials container is attached at the back of the PV system.

In this article we have reported the effect of phase change materials on BICPV performance and its potential to regulate photovoltaic temperature. A BICPV-PCM system has been modeled and simulated using a Multiphysics engineering software package. A parametric study has been conducted for the ambient temperature effect.

NUMERICAL APPROACH

Model Case Description

The modeled BICPV-PCM system (figure 2) consists of 5 Laser Grooved Buried Contact (LGBC) crystalline silicon cells. Each solar cell is 116mm long and 6 mm wide. The solar cells are connected electrically in series with highly conductive thin strips. Sylgard 184 encapsulation has been used to fix the concentrator to the solar cell and keep the solar cell surface clean. A linear asymmetric compound parabolic concentrator (LACPC) with a concentration ratio of 3 suns is used. An aluminum plate is placed beneath the solar cell to discharge the heat from the solar cells, Kapton tape is used for electrical insulation between the solar cells and the aluminum plate. The module geometry and properties are similar to [5].

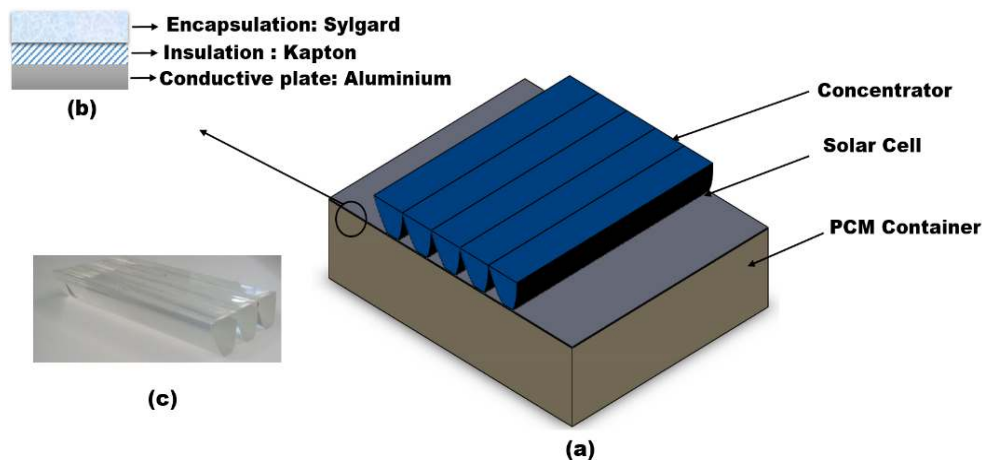


FIGURE 2. BICPV-PCM model arrangements (a) General arrangement, (b) Top cover layers, (c) Parabolic concentrator.

The above BICPV arrangement was placed in a container filled with a PCM. The container is made of thermally insulated materials (poly-methyl methacrylate). RT 31 was used as the PCM in this study. The thermo-physical properties of the simulated materials are presented in tables 1 and 2. The PCM dimension is 144mm wide and 15mm

thick. The depth of the container is much larger than the thickness, so two-dimensional analysis can be applied. In addition the following boundary conditions/assumptions were applied to simplify the problem:

1. The solar cell efficiency is constant (19%).
2. The total solar radiation transmitted to the solar cell is 90% of solar irradiation collected by the concentrator.
3. PCM flow is laminar, incompressible and Newtonian.
4. The PCM is pure, homogeneous, and isotropic.
5. The melting process occurs over a range of phase transition temperature ($2\Delta T$)
6. All the PCM container sides are adiabatically insulated.
7. The ambient temperature is 22°C .
8. The top side convection heat transfer coefficient is $5.8\text{W}/\text{m}^2\text{K}$ and it is $9.5\text{W}/\text{m}^2\text{K}$ in the bottom.

TABLE 1. Thermo-physical properties of PCM used in model

Property Name	Units	Value
Heat Capacity	C_p (J/kg.K)	2000
Density(solid)	ρ_s (kg/m ³)	880
Density(Liquid)	ρ_l (kg/m ³)	760
Viscosity	μ_l (kg/m.s)	1.789×10^{-3}
Melting Temperature(main Peak)	T_m ($^\circ\text{C}$)	31
Thermal Conductivity	k (W/m.K)	0.2
Latent heat of fusion	L (J/kg)	170

TABLE 2. Geometry and thermo-physical properties of BICPV components

Property Name	Solar Cell	Concentrator	Front and Back plate	Dielectric Layer	encapsulation
Material	Silicon	Acrylic	Aluminum	Kapton tape	Sylgard
ρ (kg/m ³)	2329	1162	2700	1530	1030
k (W/m.K)	149	0.1875	238	0.12	0.27
C_p (J/kg.K)	900	1465	900	1000	1030
Thickness(mm)	0.3	-	0.6	0.065	0.5

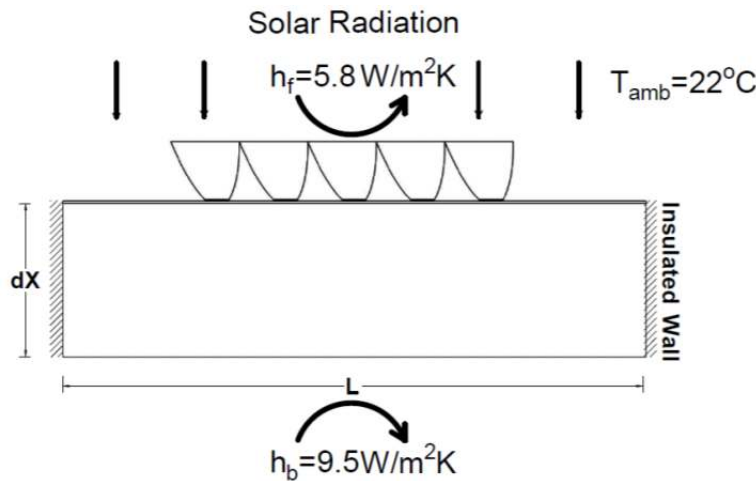


FIGURE 3. Main model boundary conditions

Mathematical Model

Modeling heat transfer

A comprehensive mathematical model for PCM heat transfer analysis has been developed by Biwole et al [8- 9]. This includes the heat transfer and fluid flow. The total heat generated by the solar cell (Q_h) is modeled as heat source and can be expressed as:

$$Q_h = (1 - \eta_{elec}) Q_o \quad (1)$$

Where Q_o indicates the optical power in W/m^2 at the outlet of the concentrator and η_{elec} is the electrical efficiency of the solar cell. The optical power takes into the account both the concentration ratio and the concentrator efficiency.

The heat transfer in solar cell is given by:

$$\rho C_p \frac{\partial T}{\partial t} + k \frac{\partial T}{\partial x} + h(T_{amb} - T) = Q_h \quad (2)$$

Where ρ is the density (kg/m^3), C_p is the heat capacity ($J/kg K$), k is the material's thermal conductivity ($W/m K$), h is the convective heat transfer coefficient ($W/m^2 K$) and T_{amb} is the ambient temperature.

The heat transfers diffusion equation applies over the PCM and can be expressed as:

$$\rho C_p \frac{\partial T}{\partial t} + \nabla \cdot (-k \nabla T) + \rho C_p \vec{u} \cdot \nabla T = 0 \quad (3)$$

Where \vec{u} is the velocity given by Navier-stokes equations for incompressible fluids. The changes in the PCM therm-physical properties occur during the phase transition stage and this is expressed by defining liquid fraction in the PCM domain:

$$B(T) = \begin{cases} 0, & T < (T_m - \Delta T) \\ \frac{T - T_m + \Delta T}{2\Delta T}, & (T_m - \Delta T) \leq T < (T_m + \Delta T) \\ 1, & T > (T_m + \Delta T) \end{cases} \quad (4)$$

Where ΔT is the melting temperature range. Therefore, the PCM thermo-physical properties are as follow:

$$\rho(T) = \rho_{solid} + (\rho_{liquid} - \rho_{solid}) \cdot B(T) \quad (5)$$

$$k(T) = k_{solid} + (k_{liquid} - k_{solid}) \cdot B(T) \quad (6)$$

$$C_p(T) = C_{p\ solid} + (C_{p\ liquid} - C_{p\ solid}) \cdot B(T) + L \cdot D(T) \quad (7)$$

Where ρ is the density, k is the thermal conductivity, C_p is the specific heat and L is the latent heat of fusion of the PCM. $D(T)$ is a smoothed Gaussian function which is zero everywhere except in the melting interval and is expressed as:

$$D(T) = \frac{e^{-(T-T_m)^2/(\Delta T)^2}}{\sqrt{\pi} \cdot \Delta T} \quad (8)$$

In this model, the PCM is assumed to be in liquid phase. The mass, momentum and energy conservation equations are coupled with the heat transfer diffusion.. The momentum conservation equation is modified to model the phase change using two forces: buoyancy force (F_b) and the force to control the solid phase (F_a). These are expressed as follows:

$$\vec{F}_b = -\rho_{solid} (1 - \beta(T - T_m)) \vec{g} \quad (9)$$

$$\vec{F}_a = -A(T) \vec{u} \quad (10)$$

Where β is the coefficient of thermal expansion (K^{-1}) and $A(T)$ is expressed as:

$$A(T) = \frac{-C(1-B(T))^2}{(B(T)^3 + q)} \quad (11)$$

Where C and q are constants and equal to 10^5 and 10^{-3} respectively.

RESULTS AND DISCUSSIONS

The modeling of the BICPV-PCM system presented here allows us to determine the temperature, fluid movement, PCM melting profiles and fraction at any point during the simulation time period. The BICPV-PCM system is dependent on climatic conditions such as solar radiation intensity, ambient temperature and wind speed. Therefore, geographic regions with different climate conditions will need specific designs and should be treated individually. The BICPV system without PCM is analyzed first in order to identify the solar cell and concentrator temperature requirements for the PCM type.

The Predicted BICPV Thermal Behavior for Different Solar Radiation Intensity

BICPV simulations without a PCM were undertaken for 200, 400, 600, 800 and 1000 W/m^2 for 3 suns. The simulations were executed using time dependent model in order to establish the time required for the system to reach the steady state condition. The predicted average PV surface temperatures and average concentrator temperature are shown in figure 4. The solar cell temperature increases as the solar radiation increases. Due to the low thermal conductivity of the concentrator materials, the difference between the solar cell temperature and the top concentrator temperature also increases. In addition, the solar cell reaches its steady state average temperature faster than the concentrator.

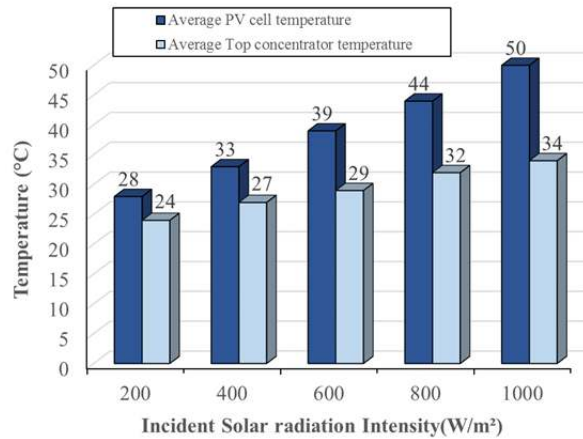


FIGURE 4. The predicted concentrator and solar cells average temperature for the BICPV system for different solar radiation intensity.

The modeled solar cell has a maximum efficiency of 19% under the standard conditions for CPV modules, which are a DNI of 1000 W/m^2 and 25 $^{\circ}C$. For similar solar cells, [10] has reported that the cell efficiency dropped at a rate of 0.3% per degree temperature rise. Therefore, the solar cell efficiency decreases with solar radiation intensity for 200,400,800 and 1000 W/m^2 at rate of 1%, 2%, 4%, 6% and 7% respectively. Thus, the BICPV system temperature for solar radiation intensity of less than 600 W/m^2 and a 22 $^{\circ}C$ ambient temperature can be managed using a simple passive heat sink

The Predicted Thermal Behavior for the BICPV-PCM System

The simulation results obtained for the BICPV-PCM system are presented in this section. The results focused on the faces temperature (concentrator and solar cells), PCM melted fraction and the surface thermal \melting profiles.

The considered solar radiations were 600 and 800 W/m² at an ambient temperature of 22°C. This range of solar radiation is the maximum range that can be reached in the UK for long periods. Figure 5 shows the predicted front concentrator average temperature and solar cells average temperature. Initially, the solar cell temperature increases rapidly for both cases until it reaches 31°C (the PCM melting temperature). After this point, the PCM starts melting and is able to absorb the heat in latent form. The time lag between the start of PCM melting point and the solar cell stabilization temperature is due to the low thermal conductivity of the PCM and the melting occurs in a range of temperature.

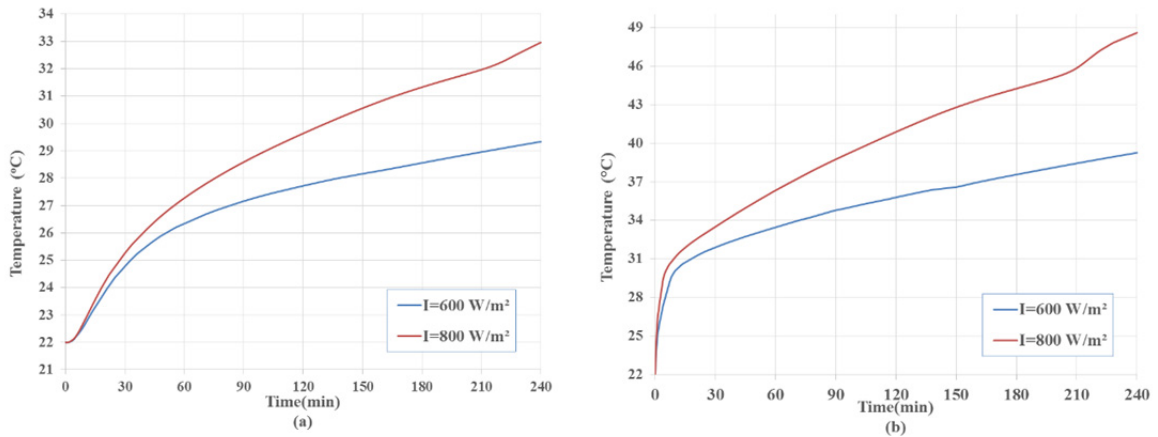


FIGURE 5. The predicted average temperature versus times, ambient temperature 22°C for different solar radiation intensity (a) Concentrator average temperature, (b) Solar cells average temperature.

The isotherms surface plots shows a straight horizontal line melting patterns. This is explained due to the low PCM thickness and thermal conductivity which allows more time for heat to spread across the PCM. The predicted PCM melting fraction is shown in figure 6. The PCM does not melt completely for 600W/m² solar radiation intensity during the simulation period. For 800W/m² solar radiation intensity, the PCM melted completely after 204 minutes. This explains the increase of temperature slope line in figure 5 for 800W/m² after this time.

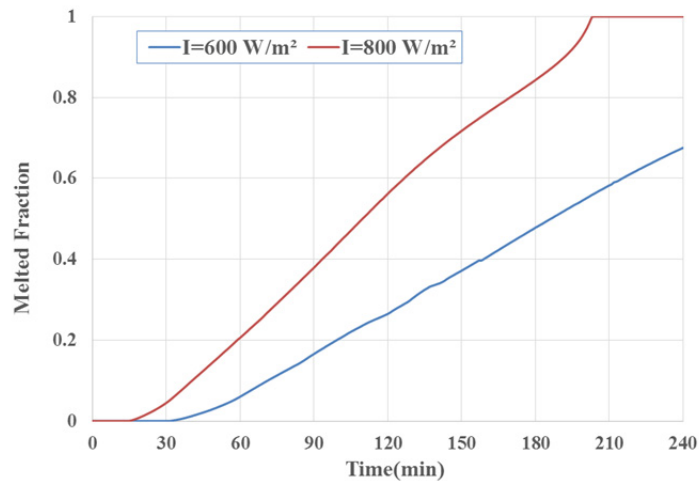


FIGURE 6. The predicted PCM melting fraction versus time, ambient temperature 22°C for different solar radiation intensity.

As stated earlier, the main objective of the PCM is to regulate the solar cell temperature. In order to find its effect in the system, the solar cells temperature difference has been calculated for BICPV and BICPV-PCM systems as shown in figure 7. The positive temperature value indicates that the solar cells experience less temperature in the system with PCM. The maximum temperature difference between the two systems occurs just before the materials

starts melting. Once melting starts, the temperature difference reduces. It can be seen that the maximum temperature difference of 800W/m^2 is 10°C which corresponds to 3% efficiency improvement. Also, the figure shows that solar cell temperature in BICPV-PCM system is higher than in no-PCM system for 600W/m^2 and 800W/m^2 after 220 minutes and 180 minutes respectively.

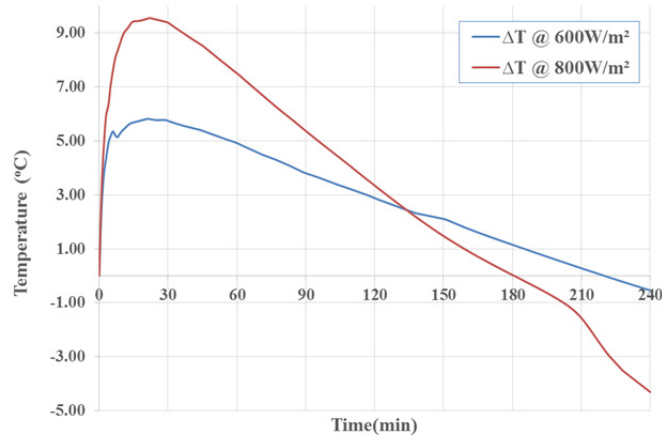


FIGURE 7. The predicted Difference of solar cells temperature BICPV with PCM and without PCM versus time, ambient temperature 22°C for different solar radiation intensity.

BICPV-PCM Thermal Behavior for Different Ambient Temperature

Natural convection plays an important role of cooling the solar cell and it directly depends on the ambient temperature. The effect of the ambient temperature on BICPV-PCM system has been studied using two different ambient temperatures: 20°C and 22°C . Figure 8 shows the predicted concentrator average temperature and solar cells average temperature at the different ambient temperatures and solar radiation intensity. As expected, the ambient temperature has an effect in reducing the system temperature. The temperature difference increases with time for both the concentrator surface temperature and solar cell temperature.

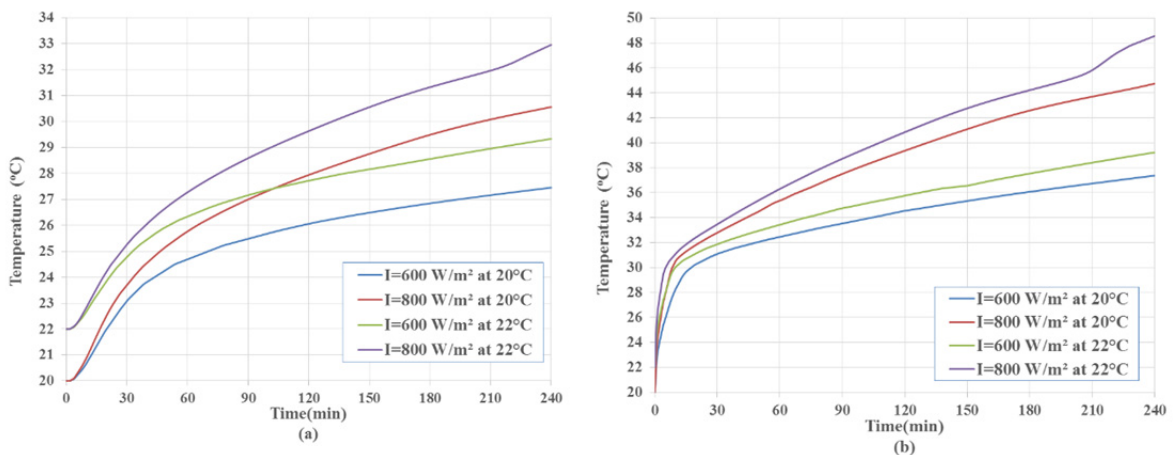


FIGURE 8. The predicted average temperature versus time for different ambient temperatures and solar radiation intensity (a) Concentrator temperature, (b) solar cell temperature.

Figure 9 shows the melting fraction for both 600W/m^2 and 800W/m^2 for different ambient temperatures. It can be noticed that the complete PCM melting in solar intensity of 800W/m^2 could be delayed half an hour if the ambient temperature decreases by two degrees. This result shows the importance of the climate conditions on the system and to be taken in consideration during the system design stage.

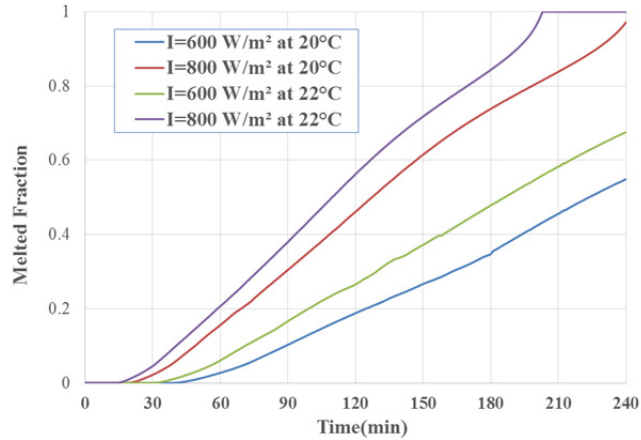


FIGURE 9. The predicted PCM melting fraction versus time for different ambient temperatures and solar radiation intensity.

CONCLUSION

The numerical model analysis of BICPV-PCM model for low CPV concentration application has been presented. The concentrator effects has been included in the model for accurate results. The heat transfer from the BICPV to the phase change material has been analyzed numerically. The results shows PCM is able to reduce/delay the solar cells temperature in certain conditions.

ACKNOWLEDGMENT

The PhD scholarship of Idris Al Siyabi is funded by the Ministry of Higher education at the Sultanate of Oman as part of the national program of postgraduate scholarships.

REFERENCES

1. O. Z. Sharaf and M. F. Orhan, "Concentrated photovoltaic thermal (CPVT) solar collector systems: Part I – Fundamentals, design considerations and current technologies," *Renew. Sustain. Energy Rev.*, vol. 50, pp. 1500–1565, 2015.
2. J. G. Ingersoll, "Simplified Calculation of Solar Cell Temperatures in Terrestrial Photovoltaic Arrays," *J. Sol. Energy Eng.*, vol. 108, no. 2, pp. 95–101, 1986.
3. B. P. Rand, J. Genoe, P. Heremans, and J. Poortmans, "Solar Cells Utilizing Small Molecular Weight Organic Semiconductors," *Prog. Photovolt Res. Appl.*, vol. 15, no. April 2012, pp. 659–676, 2007.
4. A. ROYNE, C. DEY, and D. MILLS, "Cooling of photovoltaic cells under concentrated illumination: a critical review," *Sol. Energy Mater. Sol. Cells*, vol. 86, no. 4, pp. 451–483, 2005.
5. S. Sharma, A. Tahir, K. S. Reddy, and T. K. Mallick, "Performance enhancement of a Building-Integrated Concentrating Photovoltaic system using phase change material," *Sol. Energy Mater. Sol. Cells*, vol. 149, pp. 29–39, 2016.
6. J. A. Duffie and W. A. Beckman, *Solar engineering of thermal processes*. Wiley New York etc., 1980.
7. Y. A. Cengel, S. Klein, and W. Beckman, *Heat transfer: a practical approach*. McGraw-Hill New York, 1998.
8. P. Biwole, P. Eclache, and F. Kuznik, "Improving the Performance of Solar Panels by the Use of Phase-Change Materials," *World Renew. Energy Congr.*, pp. 2953–2960, 2011.
9. P. H. Biwole, P. Eclache, and F. Kuznik, "Phase-change materials to improve solar panel's performance," *Energy Build.*, vol. 62, pp. 59–67, 2013.
10. H. Baig, N. Sarmah, K. C. Heasman, and T. K. Mallick, "Numerical modelling and experimental validation of a low concentrating photovoltaic system," *Sol. Energy Mater. Sol. Cells*, vol. 113, pp. 201–219, 2013.